Journal of Luminescence 171 (2016) 221–225

Contents lists available at ScienceDirect

Journal of Luminescence

journal homepage: www.elsevier.com/locate/jlumin

Full Length Article

High resolution spectroscopy of the $^7F_0 \leftrightarrow {}^5D_0$ transition in Eu^{3+}:KYF_4

J.G. Bartholomew [a,*], Z. Zhang [b], A. Di Lieto [b,c], M. Tonelli [b,c], Ph. Goldner [a]

[a] PSL Research University, Chimie ParisTech – CNRS, Institut de Recherche de Chimie Paris, 75005 Paris, France
[b] Dipartimento di Fisica, Università di Pisa, Largo B. Pontecorvo 3, I-56127 Pisa, Italy
[c] NEST Istituto di Nanoscienze CNR, Piazza S. Silvestro 12, I-56127 Pisa, Italy

ARTICLE INFO

Article history:
Received 12 October 2015
Received in revised form
18 November 2015
Accepted 20 November 2015
Available online 2 December 2015

Keywords:
Eu^{3+}:KYF_4
Photon echoes
Dynamic disorder modes
Electron–phonon interactions

ABSTRACT

In this paper we report the inhomogeneous and homogeneous linewidths of the $^7F_0 \leftrightarrow {}^5D_0$ optical transition for a number of sites in Eu^{3+}:KYF_4. The high frequency resolution obtained in our measurements enabled a sixth europium site to be identified, which was previously unresolved. In addition, preliminary hole burning measurements allow a partial characterization of the ^{153}Eu isotope hyperfine spin states for two sites and an approximation of the ground-state spin-level lifetime. We also discuss the temperature dependence of the homogeneous linewidth, which was measured by a two-pulse photon echo study. This study is the first photon echo measurement reported for Eu^{3+} ions in fluoride crystals. The results demonstrate that the low temperature homogeneous broadening is not limited by magnetic contributions but rather by dynamic disorder modes. These measurements also reveal electron–phonon interactions that are significantly different to oxide crystals.

1. Introduction

The extremely narrow optical transitions observed in many single crystals containing rare-earth ions continue to provide impetus for detailed spectroscopic analysis of this broad class of materials. Solid-state materials possessing narrow linewidths are promising candidates for a number of applications including classical signal processing [1,2], laser locking [3,4], spectral filtering [5], and quantum state storage [6–8]. Over the last two decades efforts toward understanding and applying narrow optical transitions in rare-earth-ion crystals have focused predominantly on oxides. Oxide crystals are appealing because the homogeneous broadening due to magnetic interactions between the rare-earths and other ligands in the crystal can be as low as 50 Hz [9].

Whilst not as extensively studied as oxides in recent times, single crystal fluorides containing rare-earth ions are another interesting category of materials for investigating narrow optical transitions. Many early studies of the energy levels of rare-earth ions in crystals and non-linear spectroscopy were performed in fluoride crystals (see, for example, Ref. [10]). Fluoride crystals have the lowest inhomogeneity of any rare-earth materials measured to date [11] and control of the fluorine nuclear-spin flips can allow optical broadening to approach the lifetime limit [12,13]. Furthermore, there is a large industry devoted to continually improving the growth of high quality fluoride crystals for a variety of applications in the field of optics.

Of the rare-earth fluorides, crystals containing impurity levels of europium are particularly interesting. In such materials the $^7F_0 \leftrightarrow {}^5D_0$ transition is only very weakly allowed, which leads to the $^5D_0$ optical excited state possessing a lifetime T_1 as long as 22.5 ms [14]. Therefore, there is the potential to achieve optical transitions with broadening less than 10 Hz if the europium ions can be decoupled from other perturbations in the crystalline environment. For example, the dominant perturbation in many fluoride crystals is the magnetic field fluctuations resulting from resonant fluorine spin flips. By applying techniques to reduce the magnitude of these magnetic fluctuations and reduce the europium ion's sensitivity to magnetic fields [13,15], it should be possible to reduce the homogeneous linewidth toward the lifetime limit.

To date, the contributing broadening mechanisms in europium doped fluoride crystals have yet to be studied in detail. In this paper we report the results of high resolution optical spectroscopy performed on a 0.1% Eu^{3+}:KYF_4 single crystal where we study the broadening mechanisms acting on the $^7F_0 \leftrightarrow {}^5D_0$ transition of two europium sites. We measure the homogeneous linewidths of the Eu^{3+} optical transitions using a two-pulse photon echo study. To our knowledge, this is the first time that photon echoes have been reported in Eu^{3+}-doped fluoride crystals. Through the sub-kHz resolution this technique provides and by measuring the temperature dependence of the homogeneous linewidth, we

* Corresponding author.
E-mail address: john.g.bartholomew@gmail.com (J.G. Bartholomew).

http://dx.doi.org/10.1016/j.jlumin.2015.11.025
0022-2313/

demonstrate that rather than being limited by magnetic interactions, the broadening of the transition is dominated by disorder modes in the crystal.

2. Background

Single crystals of KYF_4 have a trigonal, non-centrosymmetric structure where the cations are arranged in an *abc* sequence perpendicular to the *c*-axis [16]. The three cationic layers consist of alternating chains of YF_7 and KF_8. In total there are six Y^{3+} sites, all with C_1 point group symmetry, that are divided into two subclasses of three sites. The subclasses are defined by the differing pentagonal bipyramids formed by the F^- surrounding the Y^{3+} site.

There are a host of studies performed for KYF_4 containing rare-earth ions (for example [17–22]) motivated by the search for efficient laser materials. In contrast, there are very few papers on the Eu^{3+}-doped material [23,24]. The previous work in these materials studied the excitation spectra of 1% Eu^{3+}:KYF_4 crystals and measured the excited state lifetimes. Some of these results are summarized in Table 1. Notably, in the optical spectroscopy presented in Refs. [23,24], only five of the possible six Eu^{3+} sites have been identified.

3. Experimental

A 0.1% Eu^{3+}:KYF_4 crystal was grown by the Czochralski technique in the Pisa growth facility. The starting materials were powders of EuF_3/YF_3 and KYF_4 with 5 N purity (99.999%), provided by AC Materials (Tampa, FL, USA). The crystal was grown in a controlled atmosphere composed of a mixture of high purity (5 N) argon and CF_4 in a furnace that had been baked at 1000 °C under vacuum prior to the growth. The pulling rate was 0.5 mm/h, the rotation rate was 5 rpm, and the temperature of the melt was computer-controlled between 825 °C and 835 °C to maintain a constant boule diameter. The seed for the growth was an undoped KYF_4 monocrystal oriented along the *c*-axis. The resultant crystal was free of internal cracks, microbubbles or inclusions. A structural analysis was performed by Laue X-ray diffraction, which confirmed that the growth produced a single crystal, and measured the orientation of the boule with respect to the crystallographic axes.

The investigated sample was a rectangular prism with dimensions 10.3 mm($\parallel a$) × 4.4 mm × 4 mm($\parallel c$) with the polished faces perpendicular to the crystal axes. A Coherent 899 dye laser was tuned to the resonant wavelengths of the $^7F_0 \leftrightarrow {}^5D_0$ transitions of the Eu^{3+} around $\lambda = 578$ nm (518.67 THz). The light was gated and modulated using an acousto-optical modulator (AOM) in a double pass configuration and focused onto the sample using a 50 mm focal length lens. The sample was mounted in a helium bath cryostat such that the beam propagation was along the 10.3 mm *a*-axis of the crystal. The transmitted beam was gated by a further AOM and focused onto an avalanche photodiode. Fluorescence from the sample was also collected at right angles to the excitation beam and the emission spectrum was analyzed through the use of a grating spectrometer.

Table 1
Properties of the $^7F_0 \leftrightarrow {}^5D_0$ transition for different sites in Eu^{3+}:KYF_4. The site labels are taken from Ref. [24]. The resonant frequency is the center frequency of the inhomogeneous line as measured in our experiment. The † denotes that site A was not observed in our measurements and so the frequency given is that measured in Ref. [24]. The lifetimes measured by Khaidukov et al. are included next to the results of our measurements.

Site	Resonant frequency (THz)	Lifetime (ms)	Inhomogeneous linewidth (GHz)	Homogeneous linewidth (kHz)
A	519.31†	–	–	–
B	519.110 (i), 519.095 (ii)	10.6 (8.3 [23])	3.5 (i), 3.5 (ii)	–
C	519.024	– (8.3 [23])	3.4	–
D	518.069	8.3 (8.4 [23])	3.1	20.1
E	517.957	8.3 (7.8 [23])	2.6	17.5

4. Results and discussion

4.1. Inhomogeneous linewidths

The excitation spectrum of the Eu^{3+}:KYF_4 crystal at 25 K between 578.9 nm (517.9 THz) and 577.4 nm (519.2 THz) is shown in Fig. 1. More detailed plots of the five transitions that were observed within this excitation region are also shown in the figure insets. We label the transitions according to the naming convention used by Jang et al. [24]. Transitions D and E are resonant near 518 THz and correlate closely in frequency and relative intensity to the transitions observed in Refs. [23,24]. The emission intensity from both these transitions was strongly dependent on the excitation polarization, which was rotated in a plane perpendicular to the *a*-axis. The maximum fluorescence level was observed when the polarization was parallel to the *c*-axis of the crystal.

The transitions resonant near 519 THz (B and C) also correlate with previously reported transition frequencies. Notably, no transition near 577.29 nm (519.3 THz) was observed in fluorescence, which differs from the previous work by Jang et al. [24]. This difference is likely to be the result of the lower concentration of the sample investigated in this work. In contrast to transitions D and E, no polarization dependence of the emission intensity was observed for sites B and C when the polarization was rotated in a plane perpendicular to the *a*-axis.

The inhomogeneous linewidths observed in this work are approximately an order of magnitude narrower than in the study of Jang et al. who studied samples with a 1% europium concentration. One result of the narrower linewidths observed in this sample is that two transitions could be resolved around a wavelength of 577.53 nm (519.1 THz), which we label B(i) and B(ii). This suggests that transition B studied in both Refs. [23,24] is actually two transitions, which are only resolved when the inhomogeneous linewidth is sufficiently narrow.

There is strong evidence to suggest that the appearance of two resolved transitions B(i) and B(ii) reveals the sixth C_1 site

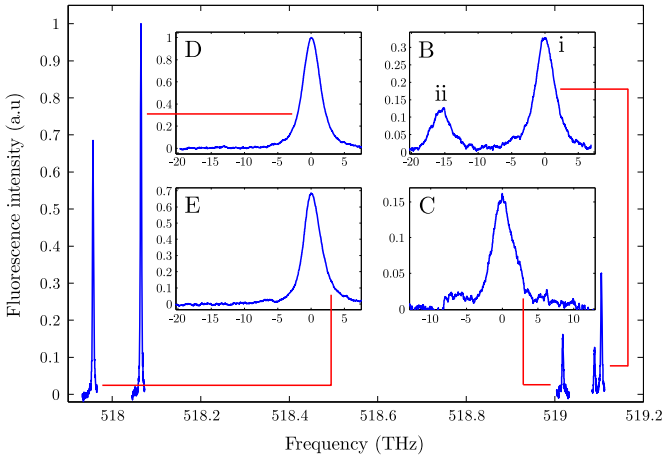

Fig. 1. Excitation spectrum of the $^7F_0 \leftrightarrow {}^5D_0$ transitions in the 0.1% Eu^{3+}:KYF_4 crystal obtained by monitoring fluorescence due to the relaxation to the $^7F_1$ states: 585 nm for sites B and C and 587 nm for sites D and E. The horizontal axes of the inset graphs are in GHz.

previously unreported for Eu^{3+}:KYF_4. In Ref. [24] the five observed transitions are divided into two groups: Group I (A, D, and E) and Group II (B and C). This division is based on the maximum energy separation between levels within the $^7F_1$ multiplet, which is $<190\,cm^{-1}$ for Group I and $>370\,cm^{-1}$ for Group II. In this work we found the $^7F_1$ splitting of the B(i) and B(ii) transitions to be $380\,cm^{-1}$ and $404\,cm^{-1}$, respectively. We therefore assign B(i) and B(ii) to Group II, which completes the identification of the six sites for Eu^{3+}:KYF_4. We also note that the observed polarization dependence of the five sites observed in our work preserves the group definitions, further supporting our conclusion.

The inhomogeneous linewidths for the five observed transitions range from 2.6 GHz for the lowest frequency site to 3.5 GHz for the highest frequency site. In all cases, the broadening is similar to high quality oxide crystals where dopant concentration broadening of the order of 20 GHz/mol% is observed [25]. For the series of five transitions observed the inhomogeneous linewidth is correlated with the transition frequency. This was also observed in Ref. [24], although with broader inhomogeneous linewidths. This suggests that there is a site dependent sensitivity to strain. It would be interesting to investigate this hypothesis further by performing detailed x-ray diffraction measurements, similar to those performed in Ref. [26], to correlate the optical transition frequencies to the crystallographic sites.

4.2. Optical hole burning spectroscopy

To probe within the inhomogeneously broadened transitions, hole burning measurements were performed on sites D and E. A burn-scan sequence was performed to create a spectral hole by optical pumping at a set frequency, which was then read out by scanning the laser 1 GHz in 250 ms. The resultant fluorescence spectra are shown in Fig. 2. The spectral resolution is limited to the order of 50 MHz by a combination of laser jitter and power broadening. This prevents much of the spectral structure from being resolved and hence, it is not possible to completely characterize the ground and excited state hyperfine parameters. Despite this, three pairs of side holes are resolved for both sites as shown in Fig. 2. This structure is most likely to be due to the excited state hyperfine structure for the ^{153}Eu isotope. The hyperfine energy splittings of the $^5D_0$ level were manually determined by identifying the frequencies at which local minima occurred symmetrically about the central hole in multiple spectra. From this analysis the excited state hyperfine splittings for the ^{153}Eu isotope are 110 ± 10 MHz and 170 ± 10 MHz for site D, and 85 ± 10 MHz and 150 ± 10 MHz for site E.

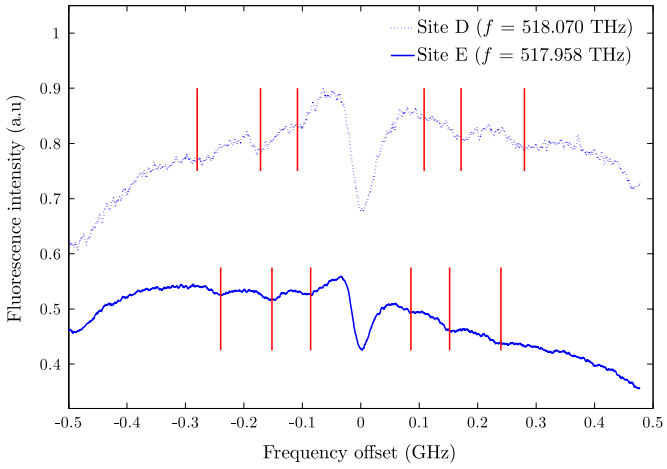

Fig. 2. Hole burning spectra for the $^7F_0 \leftrightarrow {}^5D_0$ transition in two different sites of Eu^{3+}:KYF_4. The vertical lines illustrate the central frequencies of the three pairs of side holes observed in each spectrum.

We also probed the ground state hyperfine relaxation time by burning a hole, turning off the excitation light for a set period, and then turning on the beam again to read out the hole. The holes could still be resolved on the time scale of 1 min, indicating that the hyperfine lifetime is of the order of 10 s. This is relatively short compared to the lifetimes of several days [27] to several weeks [25] observed in europium doped oxide crystals. This is not unexpected in fluoride crystals where the spin state lifetime is likely to be limited by spin–spin interactions mediated by the surrounding fluorine and yttrium spins [28].

4.3. Coherent spectroscopy

The final element of this study was to probe the homogeneous linewidth as a function of temperature for the two transitions demonstrating the strongest fluorescent signals (D and E). The detection path of the transmitted beam allowed two-pulse photon echoes to be detected using heterodyne detection [29]. For the two-pulse echo measurements the excitation power was 75 mW and the duration of the $\pi/2$ and π pulses were 3 μs and 6 μs respectively. During the measurements the laser was continuously scanned over a frequency range of 1 GHz at a rate of 100 MHz/s to avoid population depletion due to hole burning.

We can make a coarse estimate of the transition dipole moment for the two sites based on the excitation parameters that optimized the echo amplitude and by considering the equation describing the Rabi frequency Ω:

$$\Omega = \frac{\mu \cdot \mathbf{E}}{\hbar} \approx \frac{\pi}{t_\pi}, \tag{1}$$

where μ is the transition dipole moment, $\mathbf{E}$ is the electric field, and t_π is the length of a π pulse. When the polarization of the excitation pulses is aligned with the dipole moment, Eq. (1) produces

$$\mu = \frac{\hbar\pi}{t_\pi}\sqrt{\frac{cn\epsilon_0}{2}\frac{\pi R^2}{P}}, \tag{2}$$

where c is the speed of light in a vacuum, n is the refractive index, ϵ_0 is the vacuum permittivity, R is the radius of the focal spot, and P is the excitation power.

In our experiment the excitation beam was focused to a spot diameter of 100 ± 50 μm. Using $n=1.42$ for KYF_4 [17], we calculate the dipole moment of both transitions to be $\mu_{Eu^{3+}:KYF_4} = (8\pm4)\times10^{-34}\,C\cdot m^{-1}$. Therefore, the transitions measured in KYF_4 are approximately a factor of four times weaker than the $^7F_0 \leftrightarrow {}^5D_0$ transition in Eu^{3+}:Y_2SiO_5 [25]. The weak dipole moment observed in these experiments is consistent with the relatively long 8.3 ms lifetime observed for the $^5D_0$ excited state. Furthermore, the small value of μ highlights the difficulty in measuring coherent transients in similar fluoride crystals. First, high power is required to achieve the necessary pulse areas for excitation. Second, the coherent signal intensity is an order of magnitude less than commonly observed in oxide crystals because the branching ratio of the $^5D_0 \rightarrow {}^7F_0$ transition ($\approx 2\times10^{-3}$) is a factor of 10 less than in oxides [30].

Despite the weakness of the transitions, echo signals were observed that allowed the homogeneous broadening Γ_h for the D and E transitions to be studied. The results are shown in Fig. 3. At 1.8 K the homogeneous broadening was 20.1 ± 0.4 kHz and 17.5 ± 0.7 kHz for the D and E transitions respectively. The echo amplitude decayed exponentially as the delay between the two excitation pulses was increased up until 40 μs. For delays greater than 40 μs the rate of decoherence increases, which indicates the presence of spectral diffusion on this time scale. This observation

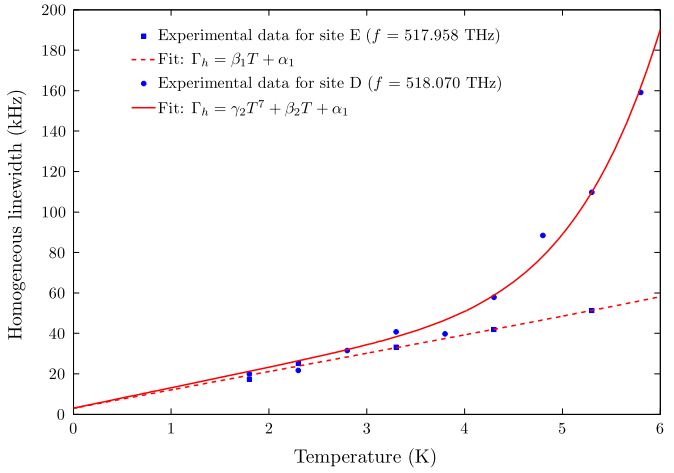

Fig. 3. Temperature dependence of the homogeneous linewidth for two different sites of Eu^{3+}:KYF_4.

warrants further study using stimulated echoes to study the spectral diffusion in detail.

To further investigate the nature of the broadening mechanism, the dependence of the homogeneous broadening Γ_h on temperature was measured. As shown in Fig. 3, the Γ_h of the two sites follow distinct temperature dependences. While the homogeneous broadening increases linearly with temperature below 6 K for site E, Γ_h for site D increases linearly at low temperature but then increases rapidly above 3.5 K. We attribute the linear component of the temperature dependent broadening of both sites to interactions between the rare-earth ion and dynamic disorder modes or, as they are also known, two-level systems (TLS) [31,32]. In contrast, the rapid broadening of site D above 3.5 K is unlikely to be due to TLS interactions, which typically contribute a linewidth proportional to T^x for $1 < x < 2.5$ [28]. Rather, the most probable mechanism for the additional broadening observed for site D is two-phonon Raman scattering, which has a characteristic T^7 dependence in bulk crystals [33].

In fitting the temperature dependent homogeneous line-width data, we assume that in the absence of broadening due to TLS and phonon processes, the underlying linewidth is the same for both sites. This underlying broadening is equivalent to the linewidth extrapolated to absolute zero, α_1, and can be considered indicative of the remaining magnetic broadening. We then jointly fit the data for site E to a linear dependence and the data for site D to the sum of a linear and a T^7 component. The fitting is optimized when the linewidth extrapolated to 0 K is $\alpha_1 = 3.0 \pm 0.5$ kHz. We note that this value is consistent with the broadening expected from the interactions between the europium and the magnetic fluctuations due to ^{19}F spin flips (of the order of 5 kHz) [34].

The fits for both sites yielded the same value for the linear broadening contribution $\beta_1 = \beta_2 = 10 \pm 1$ kHz/K. This contribution is within the range observed for the linear temperature dependence of Γ_h in anomalous crystals of Eu^{3+}:Y_2O_3 (7–15 kHz/K) [31] but significantly higher than observed in some Eu^{3+}:Y_2SiO_5 crystals (0.6 kHz/K) [32]. The cause of the dynamic disorder modes in Eu^{3+}:KYF_4 is not known. We suggest that the TLS is related to anion defects in the crystalline structure. Theoretical studies have shown that there is a relatively low energy penalty for creating anion Frenkel defects in KYF_4 [35]. Given that there is a very large number of fluorine sites (24) in the unit cell [23], the defect density could be sufficiently high to create dynamic disorder modes even in Czochralski grown crystals.

The models of Γ_h(T) for sites D and E also allow us to investigate the electron–phonon coupling in this material. From the fit of Γ_h(T) for site D, the coefficient of the T^7 component $\gamma_2 = 0.45$ Hz/K^7, whereas for site E the coefficient is less than 0.003 Hz/K^7. The value of γ_2 measured for site D is two orders of magnitude larger than the values measured in Eu^{3+}-doped oxide crystals [25,27]. In contrast, the upper bound on the T^7 coefficient for site E is of the same order of magnitude as measured in oxide crystals.

At this stage it is not possible to explain the large value of γ_2 inferred for site D. This is because

$$\gamma_2 \propto H/\Omega_D^7, \tag{3}$$

where Ω_D is the Debye temperature and H is the electron–phonon coupling constant [33]. To determine the Ω_D and H for both sites and hence, the relative contribution each of these parameters make to the large value of γ_2, further homogeneous linewidth measurements are necessary at higher temperatures.

5. Conclusion

High spectral resolution spectroscopy in low concentration Eu^{3+}:KYF_4 has revealed a number of interesting properties of this rare-earth fluoride crystal. The low doping concentration of 0.1% resulted in narrow inhomogeneous linewidths, which allowed the sixth and final europium site for the Eu^{3+}:KYF_4 structure to be identified. The homogeneous linewidths for two sites (D and E) were also measured, which are the first published photon echo measurements for Eu^{3+}-doped fluoride crystals. Although the homogeneous linewidths were narrow at 1.8 K, 20.1 kHz and 17.5 kHz respectively, the temperature dependence of Γ_h in both sites indicated that the broadening is dominated by dynamic disorder modes. Both the presence of TLS interactions and the site dependent coupling to phonons warrants further study of this material to reveal more information about physical mechanisms that will play an important role in the future applications of rare-earth-ion doped fluoride crystals.

Acknowledgments

The authors would like to acknowledge I. Grassini for her competence and care in preparing the sample. We would also like to thank Ju-hyeon Lee for providing an English translation of Ref. [24] and Sacha Welinski for assisting with the emission spectroscopy experiments. This work received funding from the European Union's Seventh Framework Programme FP7/2007-2013/ under REA Grant agreement no. 287252 (CIPRIS, People Programme-Marie Curie Actions), ANR project DISCRYS (No. 14-CE26-0037-01), Idex no. ANR-10-IDEX-0001-02 PSL⋆ and Nano'K project RECTUS.

References

[1] W.R. Babbitt, J.A. Bell, App. Opt. 33 (8) (1994) 1538.
[2] H. Linget, T. Chanelière, J.L. Le Gouët, N. J. Phys. 15, 2013.
[3] P.B. Sellin, N.M. Strickland, J.L. Carlsten, R.L. Cone, Opt. Lett. 24 (15) (1999) 1038.
[4] M.J. Thorpe, L. Rippe, T.M. Fortier, M.S. Kirchner, T. Rosenband, Nat. Photon. 5 (11) (2011) 688.
[5] Y. Li, P.R. Hemmer, C. Kim, H. Zhang, L.V. Wang, Opt. Express 16 (19) (2008) 14862.
[6] M.P. Hedges, J.J. Longdell, Y. Li, M.J. Sellars, Nature (London) 465 (7301) (2010) 1052.
[7] P. Jobez, C. Laplane, N. Timoney, N. Gisin, A. Ferrier, P. Goldner, M. Afzelius, Phys. Rev. Lett. 114 (23) (2015) 230502.
[8] M. Gündoğan, P.M. Ledingham, K. Kutluer, M. Mazzera, H. De Riedmatten, Phys. Rev. Lett. 114 (23) (2015) 230501.
[9] Y. Sun, C.W. Thiel, R.L. Cone, R.W. Equall, R.L. Hutcheson, J. Lumin. 98 (1–4) (2002) 281.

[10] R.M. Macfarlane, R.M. Shelby, R.L. Shoemaker, Phys. Rev. Lett. 43 (23) (1979) 1726.
[11] R.M. Macfarlane, A. Cassanho, R.S. Meltzer, Phys. Rev. Lett. 69 (3) (1992) 542.
[12] S.C. Rand, A. Wokaun, R.G. DeVoe, R.G. Brewer, Phys. Rev. Lett. 43 (25) (1979) 1868.
[13] R.M. Macfarlane, C.S. Yannoni, R.M. Shelby, Opt. Commun. 32 (1) (1980) 101.
[14] R.J. Hamers, J.R. Wietfeldt, J.C. Wright, J. Chem. Phys. 77 (2) (1982) 683.
[15] D.L. McAuslan, J.G. Bartholomew, M.J. Sellars, J.J. Longdell, Phys. Rev. A 85 (3) (2012) 032339.
[16] Y. Le Fur, N.M. Khaidukov, S. Aléonard, Acta Crystallogr. Sect. C—Cryst. Struct. Commun. 48 (6) (1992) 978.
[17] T.H. Allik, L.D. Merkle, B.H.T. Chai, H. Voss, G.J. Dixon, J.-L.V. Lefaucheur, R. A. Utano, J. Opt. Soc. Am. B 10 (4) (1993) 633.
[18] R.E. Peale, H. Weidner, P.L. Summers, B.H.T. Chai, J. Appl. Phys. 75 (1) (1994) 502.
[19] M. Bouffard, T. Duvaut, J.P. Jouart, N.M. Khaidukov, M.F. Joubert, J. Phys. Condens. Matter 11 (24) (1999) 4775.
[20] E. Sani, A. Toncelli, M. Tonelli, F. Traverso, J. Phys. Condens. Matter 16 (3) (2004) 241.
[21] L. Bonelli, A. Toncelli, A.D. Lieto, M. Tonelli, J. Phys. Chem. Solids 68 (12) (2007) 2381.
[22] Z. Xia, A. Arcangeli, R. Faoro, M. Tonelli, J. Optoelectron. Adv. Mater. 5 (4) (2011) 336.
[23] N.M. Khaidukov, X. Zhang, J.-P. Jouart, J. Lumin. 72–74 (1997) 213.
[24] K.H. Jang, J.H. Koo, N. Phys.: Sae Mulli. 62 (7) (2012) 750.
[25] F. Könz, Y. Sun, C.W. Thiel, R.L. Cone, R.W. Equall, R.L. Hutcheson, R. M. Macfarlane, Phys. Rev. B 68 (8) (2003) 1.
[26] Y. Le Fur, N.M. Khaidukov, S. Aléonard, Acta Crystallogr. Sect. C—Cryst. Struct. Commun. 48 (11) (1992) 2062.
[27] W.R. Babbitt, A. Lezama, T.W. Mossberg, Phys. Rev. B 39 (4) (1989) 1987.
[28] R.M. Macfarlane, R.M. Shelby, Coherent transient and holeburning spectroscopy of rare earth ions in solids, in: A.A. Kaplyanskii, R.M. Macfarlane (Eds.), Spectroscopy of Solids Containing Rare Earth Ions, North-Holland, Amsterdam, 1987.
[29] N.C. Wong, E.S. Kintzer, J. Mlynek, R.G. DeVoe, R.G. Brewer, Phys. Rev. B 28 (9) (1983) 4993.
[30] D.L. McAuslan, J.J. Longdell, M.J. Sellars, Phys. Rev. A 80 (6) (2009) 1.
[31] G.P. Flinn, K.W. Jang, J. Ganem, M.L. Jones, R.S. Meltzer, R.M. Macfarlane, J. Lumin. 58 (1–6) (1994) 374.
[32] R.M. Macfarlane, Y. Sun, R.L. Cone, C.W. Thiel, R.W. Equall, J. Lumin. 107 (1–4) (2004) 310.
[33] D.E. McCumber, M.D. Sturge, J. Appl. Phys. 34 (6) (1963) 1682.
[34] This value is obtained by scaling the ^{89}Y–Eu^{3+} coupling for Eu^{3+}:Y_2O_3 [28, p. 153] by the ratio of the magnetic moments of ^{19}F and ^{89}Y.
[35] E.M. Maddock, R.A. Jackson, M.E.G. Valerio, J. Phys. Conf. Ser. 249 (2010) 012040.